J Gastroenterol 2006; 41:971–980
DOI 10.1007/s00535-006-1883-1

Journal of Gastroenterology

© Springer 2006

Cholesterol-fed rabbit as a unique model of nonalcoholic, nonobese, non-insulin-resistant fatty liver disease with characteristic fibrosis

Mosaburo Kainuma[1], Makoto Fujimoto[1,2], Nobuyasu Sekiya[3], Koichi Tsuneyama[2,4], Chunmei Cheng[5], Yasuo Takano[2], Katsutoshi Terasawa[4,6], and Yutaka Shimada[1,4]

[1]Department of Japanese Oriental Medicine, Faculty of Medicine, University of Toyama, 2630 Sugitani, Toyama 930-0194, Japan
[2]First Department of Pathology, Faculty of Medicine, University of Toyama, Toyama, Japan
[3]Department of Frontier Japanese Oriental Medicine, Graduate School of Medicine, Chiba University, Chiba, Japan
[4]21st Century COE Program, University of Toyama, Toyama, Japan
[5]Allergy and Clinical Immunology, University of California, Davis, CA, USA
[6]Department of Japanese Oriental Medicine, Graduate School of Medicine, Chiba University, Chiba, Japan

Background. The number of patients suffering from metabolic syndrome is increasing rapidly. Metabolic syndrome causes severe pathological changes in various organs, including the liver, and its main phenotype is nonalcoholic fatty liver disease (NAFLD). NAFLD has a broad spectrum ranging from simple fatty change to severe steatohepatitis with marked fibrosis. Recently, several experimental animal models for NAFLD have been proposed. However, most were established by rather artificial conditions such as genetic alteration. In the present study, we tried to establish a unique animal model mimicking some of the physiopathological features of NAFLD using high-cholesterol-fed rabbits. ***Methods.*** Male rabbits fed with standard rabbit food containing 1% cholesterol for 8 weeks and 12 weeks were compared to controls (six rabbits/group). The weight of food was strictly restricted to 100 g/rabbit per day. ***Results.*** Body weights and fasting plasma insulin levels showed no significant differences among the groups. In contrast, characteristic fine fibrosis was extended from perivenular to pericellular areas, and microvesicular fatty change with ballooning degeneration was observed in perivenular areas in livers of the cholesterol-fed rabbits. Increase of serum cholesterol level, activation of hepatic stellate cells, and exposure to oxidative stress were also recognized. ***Conclusions.*** Cholesterol-fed rabbits share several physiopathological features of NAFLD. Because this model did not show insulin resistance or obesity, it may be useful for elucidating the mechanism of NAFLD related mainly to hyperlipidemia.

Key words: nonalcoholic fatty liver disease, hepatic stellate cell, hyperlipidemia, oxidative stress, adipocyte differentiation-related protein

Received: May 10, 2006 / Accepted: July 27, 2006
Reprint requests to: Y. Shimada

Introduction

Metabolic syndrome is a new disease entity that includes various kinds of lifestyle-related diseases such as diabetes.[1] Because the number of patients suffering from metabolic syndrome is rapidly increasing, establishment of its diagnosis, treatment, and prevention is an urgent priority.[2] Metabolic syndrome causes severe tissue damage in various organs, and its main liver phenotype is nonalcoholic fatty liver disease (NAFLD). The main disease-related factors of NAFLD are considered to be obesity, diabetes mellitus, and hyperlipidemia.[3] In these modern times, NAFLD is one of the most common chronic and progressive liver diseases in developed countries, with the number of people affected increasing rapidly.[4–7] NAFLD covers a broad spectrum, ranging from simple fatty changes to severe steatohepatitis with marked fibrosis.[8] Its progressive state is also called "nonalcoholic steatohepatitis (NASH)." Because its histopathological features are quite similar to those of alcohol-induced hepatic injury, the term "nonalcoholic" is generally used. NAFLD/NASH is known to progress to cryptogenic cirrhosis at high frequency, so early diagnosis and suitable treatment are required.[9,10] The final diagnosis of NAFLD/NASH is confirmed by liver biopsy revealing marked fatty changes with fibrosis and hepatitis.[11]

The pathogenesis of NAFLD remains obscure, although the "two hits" theory is widely accepted. In brief, excess fat accumulation in hepatocytes takes place first, and then additional activity causes NAFLD. Several candidates for the second hit have been proposed, but they remain controversial.[12–14] To clarify the etiopathogenesis of NAFLD, several animal models with or without genetic alteration have recently been presented.[15–19] Most NAFLD models previously reported are related to diabetes mellitus or obesity, showing insulin resistance. In contrast, good animal models utilizing hyperlipidemia have been very few. One article re-

ported that rats fed a high-fat diet display steatosis, inflammation, and early fibrosis in the liver.[18] These models may appear similar to those of NAFLD pathophysiologically, but the degree of fibrosis is not as prominent. It is known to be difficult to produce fibrosis in the liver of rodents, but more advanced fibrosis may be induced in other species.

Cholesterol-fed rabbits have often been used as an experimental model for cardiovascular disorders due to hypercholesterolemia and atherosclerosis.[20] Although liver steatosis has been recognized in this rabbit model, no further detailed examinations have been performed.[21–23] We have carried out a study using a particular traditional Chinese/Japanese (*kampo*) formulation that prevents the progression of atherosclerosis in cholesterol-fed rabbits.[24] Our objective was the investigation of vascular changes, but macroscopic changes of the liver (enlargement, yellowish color, partial fibrosis) were also observed. Therefore, we hypothesized that cholesterol-fed rabbits might develop changes similar to those of NAFLD. To simplify the etiological aspects, the amount of food intake was strictly controlled in all rabbits examined. In the present study, we report the detailed histopathological and serological analyses of cholesterol-fed rabbits.

Materials and methods

Animals and sample collection

Eighteen male Japanese white rabbits (10 weeks old, approximately 2 kg) were purchased from Nippon SLC (Hamamatsu, Japan) and kept in individual cages in an animal room at room temperature (23 ± 1°C) under a 12-h dark-light cycle. They were allowed an adaptation period of 2 weeks and then were randomly allocated to the following three groups (six rabbits/group): control group, fed with standard rabbit food (CR-3; CLEA Japan, Tokyo, Japan) for 8 weeks; chol-8w group, fed with standard rabbit food containing 1% cholesterol for 8 weeks; and chol-12w group, fed with standard rabbit food containing 1% cholesterol for 12 weeks. The daily diet of each animal was strictly restricted to 100 g during the study period to align final body weights. After overnight fasting, all rabbits were killed under anesthesia (pentobarbital sodium, 50 mg/kg). Blood samples were taken from the inferior vena cava. The liver was dissected directly under the perfusion of physiological saline, and the right lobe was stored for formalin fixation and freezing (–80°C). All animal-use procedures were in accordance with the Guidelines for the Care and Use of Laboratory Animals, and approved by the Committee on Animal Experimentation of the University of Toyama.

Plasma lipid and serum liver function parameters

Plasma total cholesterol (T-chol), high-density lipoprotein cholesterol (HDL-chol), low-density lipoprotein cholesterol (LDL-chol), triglyceride (TG), serum aspartate aminotransferase (AST), alanine aminotransferase (ALT), and hyaluronic acid (HA) were measured.

Plasma transforming growth factor-β1

For activation of latent transforming growth factor β1 (TGF-β1) to an immunoreactive form, plasma samples

Table 1. Effect of cholesterol-rich diet on body weight and plasma/serum laboratory parameters

Measurement	Cont	Chol-8w	Chol-12w
Body weight (kg)	3.14 ± 0.14	3.04 ± 0.07	3.38 ± 0.09
Plasma/serum			
T-chol (mg/dl)	20.7 ± 1.8	1048.0 ± 133.5*	881.8 ± 130.6*
HDL-chol (mg/dl)	10.7 ± 2.1	23.5 ± 2.5**	21.8 ± 3.4**
LDL-chol (mg/dl)	2.9 ± 1.5	1021.9 ± 135.2**	850.7 ± 129.7**
TG (mg/dl)	54.8 ± 23.3	13.2 ± 6.1	46.3 ± 15.2
Insulin (ng/ml)	1.0 ± 0.3	0.4 ± 0.1	0.7 ± 0.1
AST (IU/l)	32.3 ± 6.3	17.0 ± 7.8	26.2 ± 3.1
ALT (IU/l)	38.3 ± 7.0	23.2 ± 9.0	35.7 ± 3.1
HA (pg/ml)	43.6 ± 7.5	258.3 ± 127.3	121.5 ± 36.9
TGF-β1 (pg/ml)	592.7 ± 76.9	602.9 ± 84.72	2606.5 ± 213.0**#

Values are means ± SE ($n = 6$)
Cont, control group; Chol-8w, 8-week 1% cholesterol diet-fed group; Chol-12w, 12-week 1% cholesterol diet-fed group; T-chol, total cholesterol; HDL-chol, high-density lipoprotein cholesterol; LDL-chol, low-density lipoprotein cholesterol; TG, triglyceride; AST, aspartate aminotransferase; ALT, alanine aminotransferase; HA, hyaluronic acid; TGF-β1, transforming growth factor β1
*$P < 0.05$, **$P < 0.01$ compared with control group; #$P < 0.01$ compared with Chol-8w group

were acidified with 2.5 M acetic acid and 10 M urea, and then neutralized by adding a mixture consisting of 2.7 N and 1 M HEPES. Activated samples were diluted and measured by the quantitative sandwich enzyme immunoassay technique using recombinant human TGF-β1 soluble receptor type II as a solid precoated onto a microplate (R&D System, Minneapolis, MN, USA). Optical density was read by spectrophotometer at 450 nm. The concentration of TGF-β1 was determined on the basis of a standard curve prepared with samples of known concentrations.

Plasma insulin

The plasma insulin level was measured with a rat insulin enzyme-linked immunosorbent assay kit (Seikagaku, Tokyo, Japan).

Lipid peroxide in plasma and liver

The degree of oxidative stress in plasma and liver tissue was evaluated by the concentration of lipid peroxide (LPO). Liver samples were weighed and minced in ice-cold phosphate-buffered saline (pH 7.4), then homogenized at a ratio of 1:10 (w:v). After centrifugation of liver homogenates at 3000 *g* for 10 min at 4°C, the supernatants were collected and used for the measurement. The levels of LPO in plasma and liver tissue were evaluated with a lipid peroxidation assay kit (Determinant LPO; Kyowa Medex, Tokyo, Japan) following the manufacturer's instructions.

Histopathological and immunohistochemical examinations

Five-micrometer-thick sections of formalin-fixed and paraffin-embedded liver tissues were processed routinely for hematoxylin-eosin and Azan-Mallory staining. Frozen samples were used for lipid staining with oil red stain. Mouse monoclonal antibodies against α-smooth muscle actin (α-SMA) were purchased from DAKO Cytomation (Kyoto, Japan), and against 8-hydroxy-2′-deoxy-guanosine (8-OHdG) from the Japanese Aging Control Institute (Shizuoka, Japan). Immunohistochemical staining of α-SMA and 8-OHdG was performed on paraffin-embedded sections according to recently described methods.[12,25] For 8-OHdG immunostaining, metabolic H_2O_2 treatment was performed after primary antibody application. We evaluated the area of α-SMA-positive lesions in six ocular microscopic fields (×40 magnification) per specimen for each rabbit by using NIH Image software, expressed as the percentage of the total area of the fields.

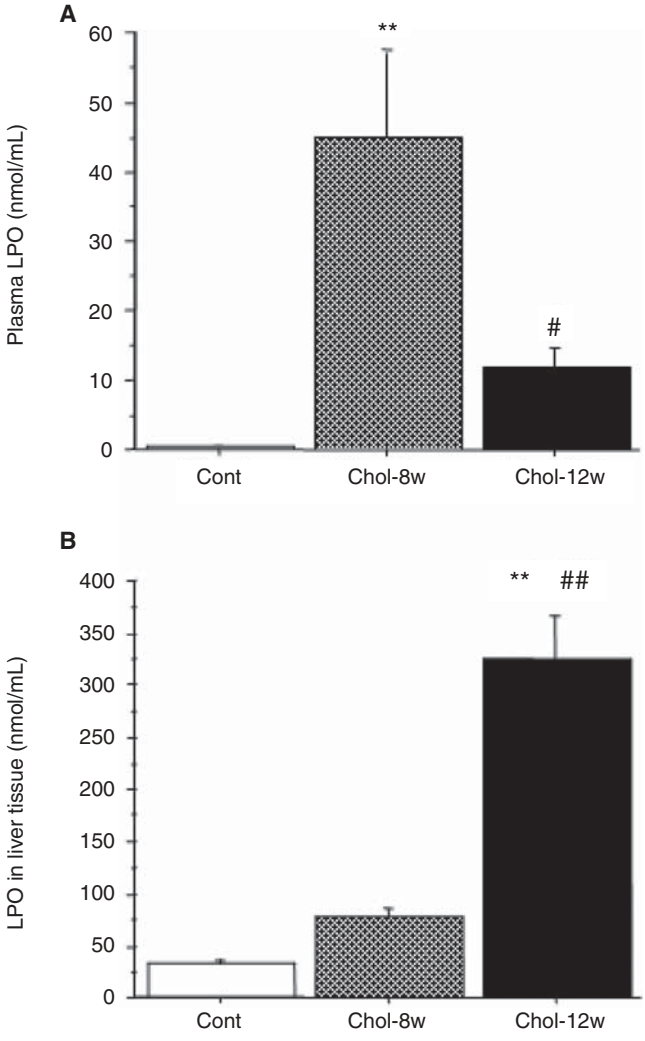

Fig. 1. Lipid peroxide (*LPO*) levels in plasma (**A**) and liver tissue (**B**). *Cont*, control group; *Chol-8w*, 8-week 1% cholesterol diet-fed group; *Chol-12w*, 12-week 1% cholesterol diet-fed group. Data are means ± SE ($n = 6$). $^{**}P < 0.01$ compared with the control group; $\#P < 0.05$, $\#\#P < 0.01$ compared with the chol-8w group

Double immunostaining for identifying hepatic stellate cells

Because of the lack of good immunohistochemical markers, hepatic stellate cells (HSCs) are not easily recognized. We focused on a new molecule, adipocyte differentiation-related protein (ADRP), which is expressed on the cell surface of lipid-laden cells. In a preliminary study, sinusoidal HSCs were clearly immunostained as well as lipid-laden hepatocytes and lipid-laden macrophages. Although the exclusion of hepatocytes is easy, it is quite difficult to differentiate HSCs and lipid-laden macrophages by morphology. To

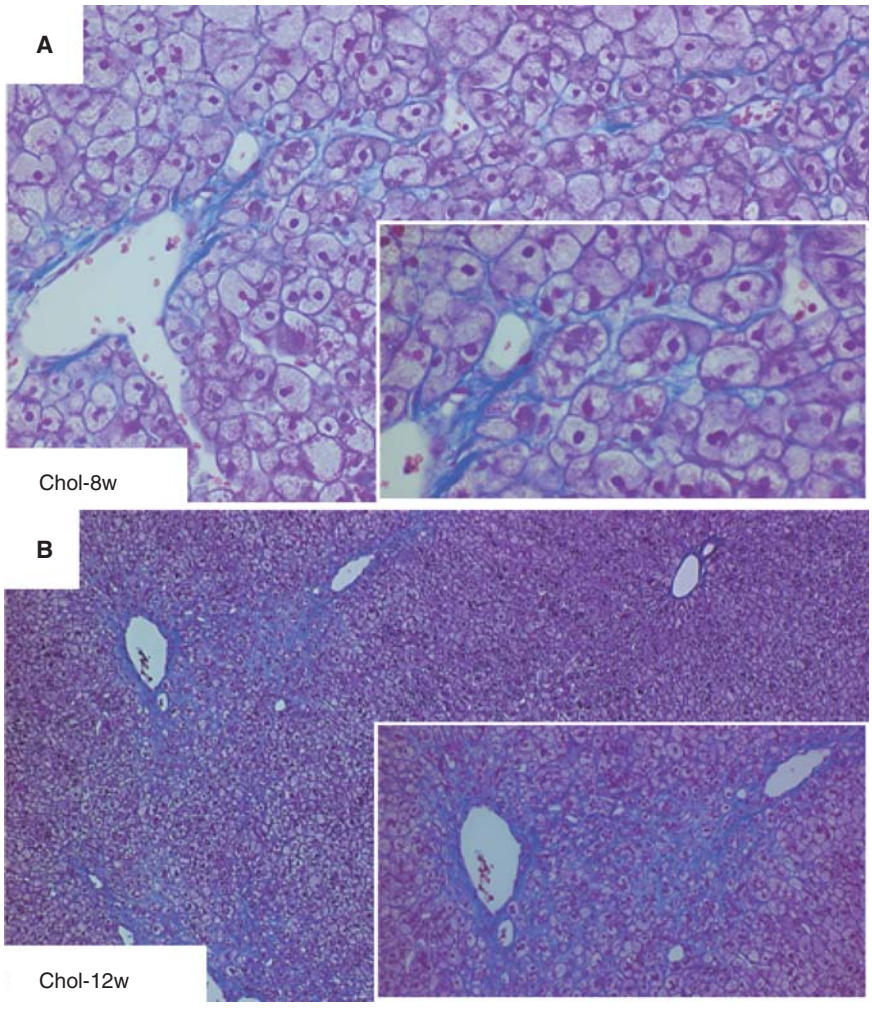

Fig. 2A,B. Histopathological findings in the livers of 8-week and 12-week 1% cholesterol diet-fed rabbits. **A** Mild fibrosis is seen from the perivenular to pericellular areas in the chol-8w rabbit (Azan-Mallory stain, original magnifications ×40 and ×200). **B** Slender and delicate fibrosis shows bridging fibrosis (C-C bridging) in the chol-12w rabbit (Azan-Mallory stain, original magnifications ×40 and ×200)

Fig. 3A–D. Histopathological findings in the livers of chol-12w rabbits. **A** Hepatocellular fat deposition is predominantly seen in the perivenular areas (oil red stain, original magnification ×40). **B** Megamitochondria (*arrows*), hepatic stellate cell aggregation and enlargement (*circles*), and microvesicular fatty changes (*arrowheads*) are observed (hematoxylin-eosin stain, original magnification ×200). **C** Hepatocellular ballooning with Mallory bodies is observed (*arrows*) (hematoxylin-eosin stain, original magnification ×200). **D** Slight infiltration of neutrophils is observed (*arrow*) (hematoxylin-eosin stain, original magnification ×200)

Fig. 4A–D. Hepatic stellate cells (HSCs) in the livers of cholesterol-fed rabbits. **A** Not only hepatocytes, which feed on fat droplets, but also HSCs in the sinusoidal area are stained orange (*arrow*) (chol-12w rabbit, oil red staining, original magnification ×200). **B** HSCs have a blue appearance in their cytoplasm; some include vacuoles in cytoplasm (*arrow*) (chol-8w rabbit, hematoxylin-eosin stain, original magnification ×200). **C** HSCs exhibit blue staining in their cytoplasm; some contain small vacuoles in cytoplasm (*arrow*) (chol-8w rabbit, Azan-Mallory stain, original magnification ×200). **D** With double immunohistochemical staining, adipocyte differentiation-related protein (ADRP) single immunostaining is strongly positive in HSCs showing brown color (*arrows*), while ADRP and macrophage double immunostaining is seen in Kupffer cells showing dark blue color (*arrowheads*) (chol-8w rabbit, original magnification ×200)

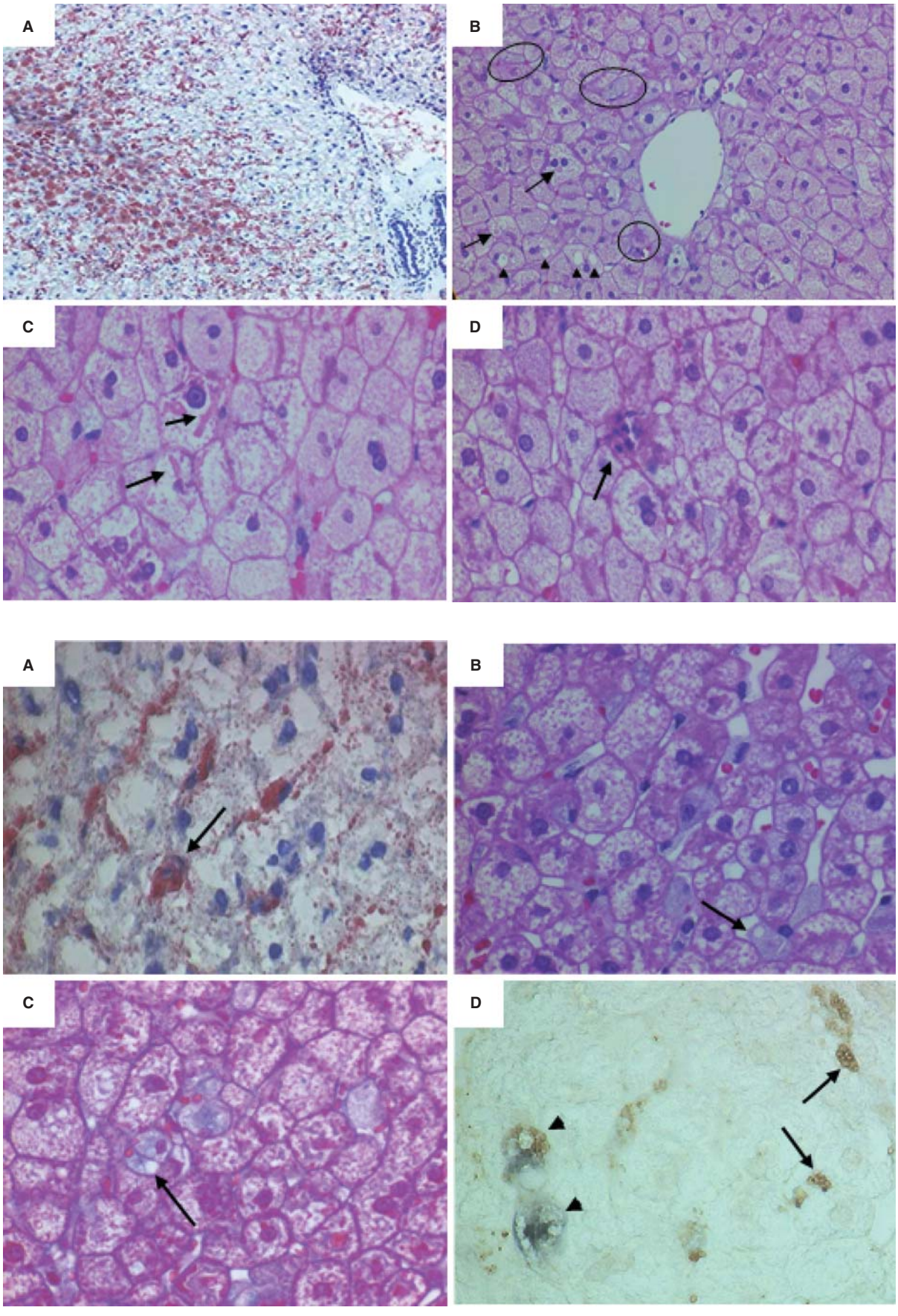
A
B
C
D
A
B
C
D

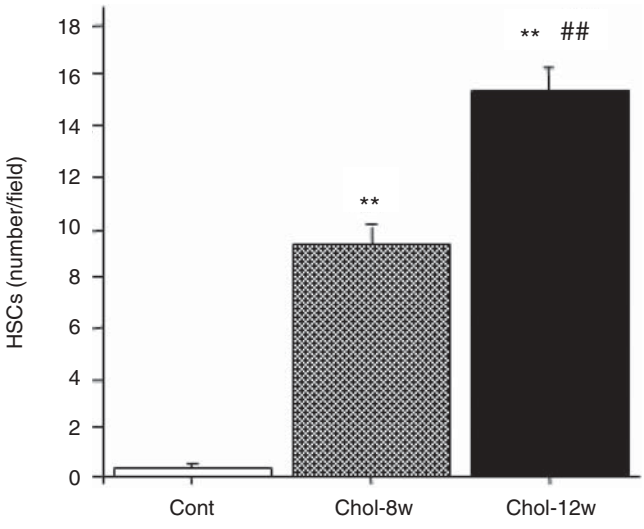

Fig. 5. Quantitative analysis of hepatic stellate cells in the livers of control, chol-8w and chol-12w rabbits. The numbers of HSCs showing single ADRP staining were counted by pathologists at ×200 magnification. Data are means ± SE ($n = 6$). $^{**}P < 0.01$ compared with the control group; $^{\#\#}P < 0.01$ compared with the chol-8w group

detect only HSCs, we designed a double-immunostaining procedure using mouse monoclonal anti-macrophage antibody (DAKO Cytomation) and mouse monoclonal anti-ADRP antibody (Progen Biotechnik, Heidelberg, Germany). In brief, ADRP was first immunostained using the Envision-PO system (DAKO Cytomation), becoming brown. After the specimens were soaked in a hot bath for 10 min, all applied antibodies were denatured. Secondary immunostaining using anti-macrophage antibody was then performed using the Envision-PO system, and positive cells were stained blue. HSCs located in the sinusoid were brown, while lipid-laden macrophages located in the sinusoid were a strong dark blue. Two pathologists counted the number of HSCs in four sinusoidal fields (×200 magnification) independently without knowledge of the animal groupings.

Statistical analysis

All values were expressed as means ± SE, and were analyzed by one-way analysis of variance (ANOVA) followed by Bonferroni's multiple comparison test. $P < 0.05$ was considered statistically significant.

Results

Laboratory parameters

There were no differences in body weight among the control, chol-8w, and chol-12w groups. T-chol, HDL-chol, and LDL-chol of both the chol-8w and chol-12w groups were significantly higher than those of the control group, but there were no differences in TG or insulin level among the three groups. Concerning the parameters of liver function and fibrosis, there were no differences in serum AST, ALT, or HA among the three groups, but the plasma level of TGF-β1 in the chol-12w group was significantly higher than those of both the control and chol-8w groups (Table 1). The plasma level of LPO in the chol-8w group was significantly higher than in the control or chol-12w groups (Fig. 1A), and the LPO level of liver tissue in chol-12w was significantly higher than in the control or chol-8w groups (Fig. 1B).

Histopathological and immunohistochemical findings

In the chol-8w rabbits, mild delicate fibrosis was seen predominantly in the perivenular to pericellular area (Fig. 2A). Although macrovesicular fatty change was not clearly distinguishable, microvesicular fat deposition and aggregation of enlarged HSCs were observed in the perivenular area, and scattered megamitochondria were observed. On the other hand, in the chol-12w group, slender fibrosis extended to form bridging (C—C bridging) in places (Fig. 2B), and hepatocellular microvesicular fat deposition was seen predominantly in the perivenular area (Fig. 3A,B). In addition, megamitochondria, enlarged-HSC aggregates, and hepatocellular ballooning with Mallory bodies (Fig. 3C) were observed, together with a slight infiltration of neutrophils (Fig. 3D). Not only hepatocytes, which feed on fat droplets, but also HSCs in the sinusoidal area were stained orange with oil red stain (Fig. 4A). In rabbit livers, HSCs were easily recognizable with various stains because of their original characteristic morphology. In cholesterol-fed rabbits, HSCs were markedly enlarged with pale cytoplasm and minute fat droplets (Fig. 4B,C). Immunohistochemical examinations clearly demonstrated ADRP expression in HSCs (Fig. 4D). In the chol-12-w group, the number of HSCs was greater. The number of HSCs in both the chol-8w and chol-12w groups was significantly higher than in the control group, and the number of HSCs in chol-12w was also significantly higher than in chol-8w (Fig. 5). Subsequent fibrosis was not observed in the livers of the control group (Fig. 6A), while it was increased in the chol-8w group (Fig. 6B). In the chol-12w group, α-SMA-immunopositive areas, which reflect the activation of HSCs, had apparently extended to the perivenular area (Fig. 6C). By computer-assisted semiquantitative analysis, the percentages of α-SMA-positive areas in the fields of both chol-8w and chol-12w groups were significantly higher than those of the control group (Fig. 6D). 8-OHdG-immunopositive cells were not apparent

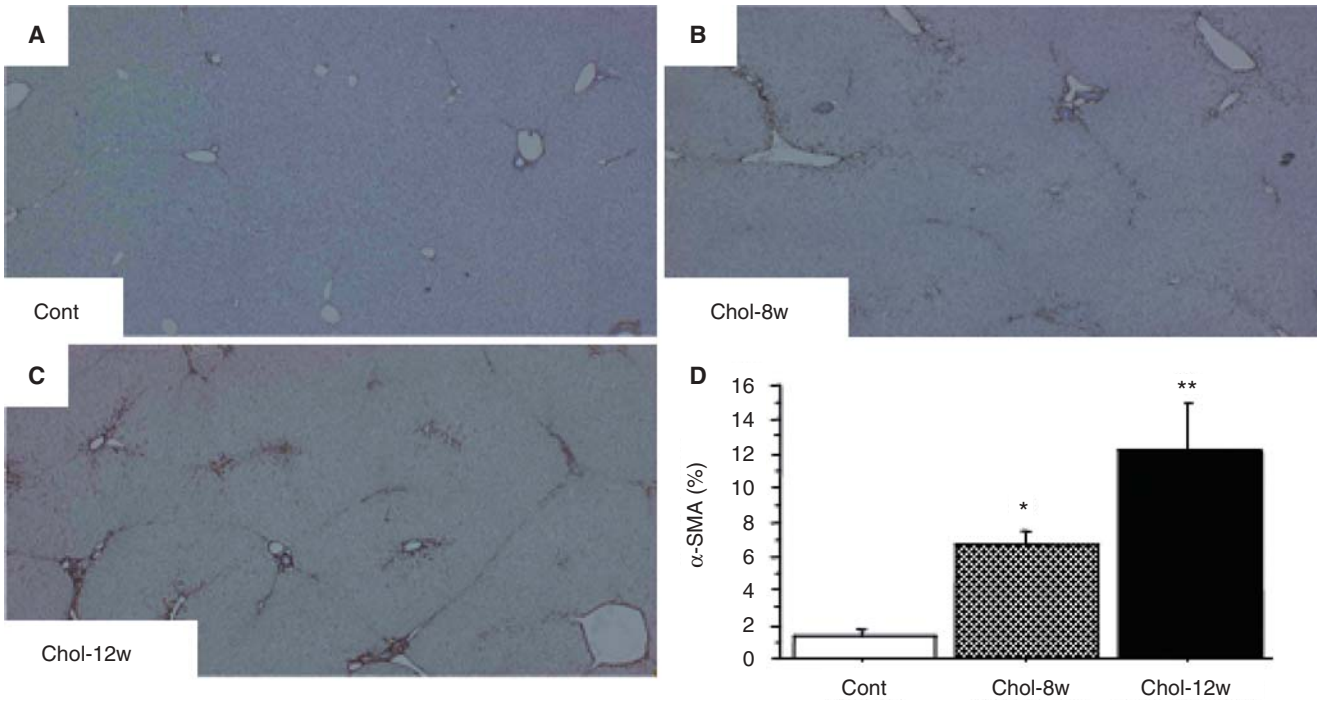

Fig. 6A–D. Immunohistochemical findings and semiquantitative analysis of α-smooth muscle actin (*α-SMA*) in the livers of control, chol-8w, and chol-12w rabbits. **A** α-SMA immunopositivity was not observed in the control rabbit (original magnification ×40). **B** α-SMA-immunopositive areas appear in the chol-8w rabbit (original magnification ×40). **C** α-SMA-immunopositive areas are extended in the perivenular area in the chol-12w rabbit (original magnification ×40). **D** Percentage of α-SMA-positive areas evaluated by computer-assisted semiquantitative analysis. Data are means ± SE ($n = 6$). *$P < 0.05$, **$P < 0.01$ compared with the control group

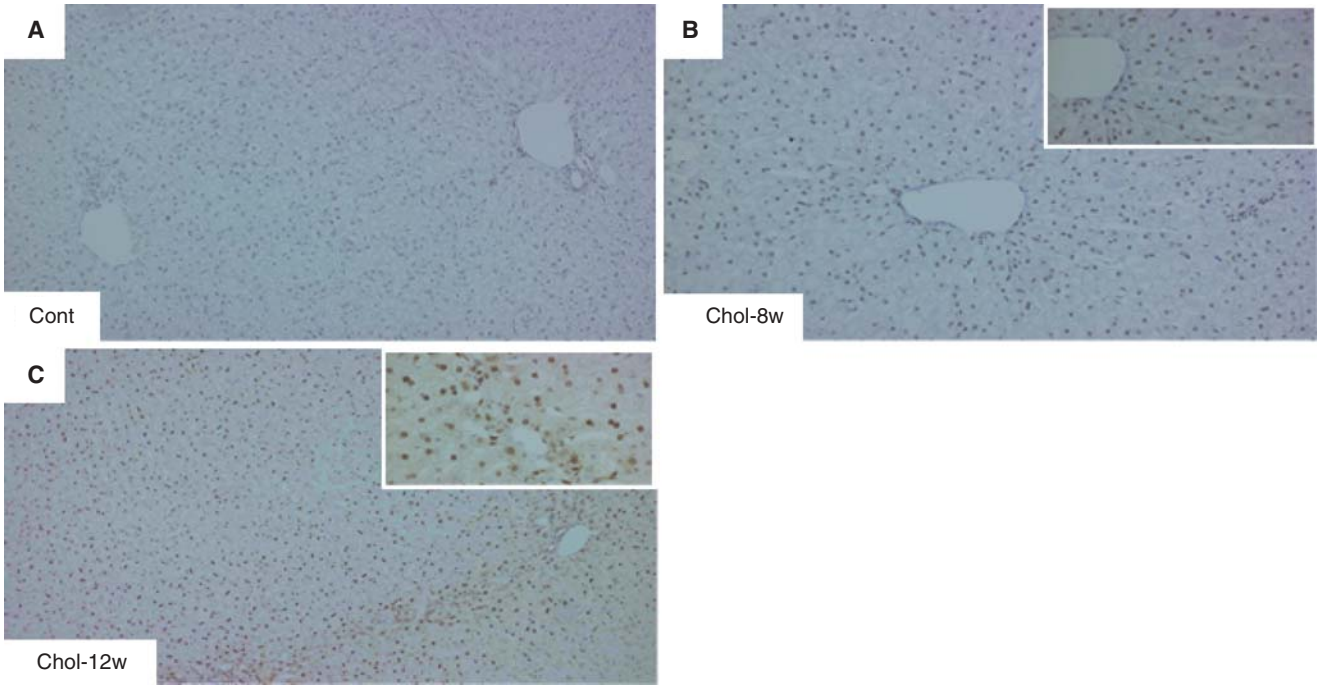

Fig. 7A–C. Immunohistochemical findings of 8-hydroxy-2′-deoxy-guanosine (8-OHdG) in the livers of control, chol-8w, and chol-12w rabbits. **A** 8-OHdG-immunopositive cells are not apparent in control rabbits (original magnification ×40). **B** Scattered and weakly positive nuclear stains are seen in chol-8w rabbits (original magnifications ×40 and ×200). **C** Scattered but densely positive nuclear stains are apparent in chol-12w rabbits (original magnifications ×40 and ×200)

in the livers of the control group (Fig. 7A), but scattered and weakly positive nuclear stains were observed in the livers of the chol-8w group (Fig. 7B). In the livers of the chol-12w group, scattered but densely positive nuclear stains were apparent (Fig. 7C).

Discussion

In the present study, we examined the serological and histopathological changes of the livers of cholesterol-fed rabbits. As expected, hepatocellular fat deposition, ballooning, slender and delicate fibrosis from the perivenular to the pericellular portions showing occasional C—C bridging, and slight neutrophil infiltration were revealed in the livers of the cholesterol-fed rabbits. In addition, the serum cholesterol level was significantly increased as expected. Although the degree of these pathological changes differed in individual rabbits, chol-12w rabbits generally suffered more severe pathological changes in the liver than chol-8w rabbits. Necroinflammatory reactions such as focal necrosis, acidophilic body, and lipogranuloma were not very prominent, but a small number of Mallory bodies and megamitochondria were observed. These liver changes were clearly caused by the special diet, as control rabbits did not show such histopathological changes.

Matteoni et al.[8] classified NAFLD into four histological subgroups, and Saadeh et al.[26] categorized NAFLD types 3 and 4 as NASH. Other investigators make a diagnosis of NASH when steatosis with ballooning degeneration or zone 3 pericellular, sinusoidal, or perivenular fibrosis appeared histologically. Although lobular inflammation and evidence of hepatocyte necrosis were noted, they are not required for the diagnosis of NASH.[27] Taking into account these reports, we consider that the chol-12w rabbits in our present study shared several physiopathological similarities with NAFLD/NASH.

The pathogenesis of NAFLD/NASH has not been fully elucidated, but the "two-hit" theory has recently received acceptance. First, excess fat accumulation occurs in hepatocytes, and then secondary activity such as oxidative stress may cause NAFLD.[13] Information from several rodent models has suggested that lipid peroxidation is an important factor in the progression of NASH.[17–19] In our chol-12w rabbits, the LPO level and 8-OHdG-positive areas in liver tissue were significantly increased compared with the other groups. Because nuclear 8-OHdG expression reflects oxidative DNA damage,[28] it was clear that pronounced oxidative stress occurred in our model. In addition, slender and delicate fibrosis extended over time with the feeding of the cholesterol diet. These results may be interpreted to indicate that our cholesterol-fed rabbits and NAFLD are caused by similar pathological processes.

Our cholesterol-fed rabbits showed microvesicular fat deposition more predominantly than the macrovesicular variety. The human form of NAFLD is characterized by a mixed macro- and microvesicular type of hepatic steatosis.[29] Macrovesicular steatosis by itself is a relatively benign condition, and is accompanied by a mild or lesser decrease of mitochondrial β-oxidation. In contrast, it has recently been clarified that microvesicular fat deposition arises whenever there is severe impairment of mitochondrial β-oxidation. Fromenty and Pessayre[30] reported that the predominant presence of microvesicular fat deposition implies a more severe condition for the body than macrovesicular fat deposition. Hypercholesterolemia might induce oxidative stress in mitochondria.

Several studies have elucidated the importance of insulin resistance in the initiation and development of NAFLD.[31–33] On the other hand, the methionine—choline deficient dietary model of steatohepatitis does not exhibit insulin resistance.[34] Our rabbit model also did not demonstrate obesity or insulin resistance. These results suggest that the etiology of NAFLD might be heterogeneous, and for this reason several animal models based on different etiologies should be examined for the establishment of prevention and treatment of NAFLD. In accordance with the role of oxidative stress in NAFLD, it has recently been reported that oxidative stress can activate HSCs directly,[35–38] and activated HSCs can produce delicate fibrosis as well as secrete TGF-β1.[38,39] In the present study, besides the oxidative stress marker in liver tissue, the number of HSCs, plasma TGF-β1 level, and α-SMA-positive areas increased over time in cholesterol-fed rabbits. With special reference to these results, we consider that our rabbit model could be helpful in elucidating the mechanism by which oxidative stress directly activates HSCs without apparent inflammation.

Quiescent HSCs are inconspicuous in the normal liver, but when activated, they are transformed into myofibroblast-like cells that produce α-SMA, and can be readily observed by immunohistochemical stains.[27] It is usually difficult to recognize quiescent HSCs because of the absence of specific immunohistochemical stains. To clarify the role of HSCs, we established an easy immunohistochemical detection system using antibodies against both ADRP and macrophages. Buyssens et al.,[22] in a transmission electron microscopy study, reported that fat-storing (stellate) cells in the liver fibrotic area of high-cholesterol-fed rabbits were irregularly shaped, enlarged, and contained fewer and smaller lipid droplets than those of control rabbits. In our cholesterol-fed rabbits, the total number of HSCs was increased. The increased number of enlarged HSCs may

parallel the progression of perivenular and pericellular fibrosis.

Compared with previous NASH models, our cholesterol-fed rabbit model has several advantages. First, high-cholesterol food is not a special diet and easily simulates human dietary habits. Second, this fatty liver disease might be caused primarily by impairment of mitochondrial β-oxidation. Third, slender and delicate fibrotic extension in the perivenular area is quite similar to that seen in NAFLD/NASH patients. Moreover, in chol-8w rabbits, while the hepatocellular damage was not so prominent, mild perivenular to pericellular fibrosis, the plasma level of LPO, and the number of HSCs in liver tissue were increased. Chol-8w rabbits might be useful for studying the very early events in NAFLD/NASH patients.

In conclusion, we reported that cholesterol-fed rabbits might represent a useful model for the analysis of some physiopathogenic aspects of NAFLD/NASH patients. Especially, the characteristic slender and delicate perivenular to pericellular fibrosis strongly resembles that of NAFLD patients. Because this model showed no obesity or insulin resistance, it may be useful in clarifying the mechanism of NAFLD resulting from hyperlipidemia.

Acknowledgments. The authors are grateful to Takako Nakagawa, Shinobu Takagi, Tokimasa Kumada, and Hideki Hatta for their technical assistance. The study was supported by a Grant-in-Aid for the 21st Century COE Program from the Ministry of Education, Culture, Sports, Science and Technology, Japan.

References

1. Hegele RA, Pollex RL. Genetic and physiological insights into the metabolic syndrome. Am J Physiol Regul Integr Comp Physiol 2005;289:663–9.
2. Bestermann W, Houston MC, Basile J, Egan B, Ferrario CM, Lackland D, et al. Addressing the global cardiovascular risk of hypertension, dyslipidemia, diabetes mellitus, and the metabolic syndrome in the southeastern United States, part II: treatment recommendations for management of the global cardiovascular risk of hypertension, dyslipidemia, diabetes mellitus, and the metabolic syndrome. Am J Med Sci 2005;329:292–305.
3. James OFW, Day CP. Non-alcoholic steatohepatitis (NASH): a disease of emerging identity and importance. J Hepatol 1998;29: 495–501.
4. Clark JM, Brancati FL, Diehl AM. Nonalcoholic fatty liver disease. Gastroenterology 2002;122:1649–57.
5. Ruhl CE, Everhart JE. Determinants of the association of overweight with elevated serum alanine aminotransferase activity in the Unites States. Gastroenterology 2003;124:71–9.
6. Bellentani S, Saccoccio G, Masutti F, Crocè LS, Brandi G, Sasso F, et al. Prevalence of and risk factors for hepatic steatosis in northern Italy. Ann Intern Med 2000;132:112–7.
7. Nomura H, Kashiwagi S, Hayashi J, Kajiyama W, Tani S, Goto M. Prevalence of fatty liver in a general population of Okinawa, Japan. Jpn J Med 1988;27:142–9.
8. Matteoni CA, Younossi ZM, Gramlich T, Boparai N, Liu YC, McCullough AJ. Nonalcoholic fatty liver disease: a spectrum of clinical and pathological severity. Gastroenterology 1999;116: 1413–9.
9. Powell EE, Cooksley WGE, Hanson R, Searle J, Halliday JW, Powell LW. The natural history of nonalcoholic steatohepatitis: a follow-up study of forty-two patients for up to 21 years. Hepatology 1990;11:74–80.
10. Bacon BR, Farahvash MJ, Janney CG, Neuschwander-Tetri BA. Nonalcoholic steatohepatitis: an expanded clinical entity. Gastroenterology 1994;107:1103–9.
11. Sumida Y, Nakashima T, Yoh T, Furutani M, Hirohama A, Kakisaka Y, et al. Serum thioredoxin levels as a predictor of steatohepatitis in patients with nonalcoholic fatty liver disease. J Hepatol 2003;38:32–8.
12. Seki S, Kitada T, Yamada T, Sakaguchi H, Nakatani K, Wasaka K. In situ detection of lipid peroxidation and oxidative DNA damage in nonalcoholic fatty liver disease. J Hepatol 2002;37:56–62.
13. Day CP, James OFW. Steatohepatitis: a tale of two "hits"? Gastroenterology 1998;114:842–5.
14. Weltman MD, Farrell GC, Hall P, Ingelman-Sundberg M, Liddle C. Hepatic cytochrome P450 2E1 is increased in patients with non-alcoholic steatohepatitis. Hepatology 1998;27:128–33.
15. Leclercq IA, Farrell GC, Schriemer R, Robertson GR. Leptin is essential for the hepatic fibrogenic response to chronic liver injury. J Hepatol 2002;37:206–13.
16. Koteish A, Diehl AM. Animal models of steatosis. Semin Liver Dis. 2001;21:89–104.
17. George J, Pera N, Phung N, Leclercq I, Yun Hou J, Farrell G. Lipid peroxidation, stellate cell activation and hepatic fibrogenesis in a rat model of chronic steatohepatitis. J Hepatol 2003;39:756–64.
18. Lieber CS, Leo MA, Mak KM, Xu Y, Cao Q, Ren C, et al. Model of nonalcoholic steatohepatitis. Am J Clin Nutr 2004;79:502–9.
19. Fan JG, Zhong L, Xu ZJ, Tia LY, Ding XD, Li MS, et al. Effects of low-calorie diet on steatohepatitis in rats with obesity and hyperlipidemia. World J Gastroenterol 2003;9:2045–9.
20. Finking G, Hanke H. Nikolaj Nikolajewitsch Antischkow (1885–1964) established the cholesterol-fed rabbit as a model for atherosclerosis research. Atherosclerosis 1997;135:1–7.
21. Gupta PP, Tandon HD, Ramalingaswami V. Cirrhosis of the liver in rabbits induced by a high cholesterol diet: an experimental model. Indian J Med Res 1976;64:1516–26.
22. Buyssens N, Kockx MM, Herman AG, Lazou JM, Van den Berg K, Wisse E, et al. Centrolobular liver fibrosis in the hypercholesterolemic rabbit. Hepatology 1996;24:939–46.
23. Wanless IR, Belgiorno J, Huet PM. Hepatic sinusoidal fibrosis induced by cholesterol and stilbesterol in the rabbit: 1. morphology and inhibition of fibrogenesis by dipyridamole. Hepatology 1996;24:855–64.
24. Sekiya N, Tanaka N, Itoh T, Shimada Y, Goto H, Terasawa K. Keishi-bukuryo-gan prevents the progression of atherosclerosis in cholesterol-fed rabbit. Phytother Res 1999;13:192–6.
25. Yoshiji H, Kuriyama S, Yoshii J, Ikenaka Y, Noguchi R, Nakatani T, et al. Angiotensin-II type 1 receptor interaction is a major regulator for liver fibrosis development in rats. Hepatology 2001;34:745–50.
26. Saadeh S, Younossi ZM, Remer EM, Gramlich T, Ong JP, Hurley M, et al. The utility of radiological imaging in nonalcoholic fatty liver disease. Gastroenterology 2002;123:745–50.
27. Washington K, Wright K, Shyr Y, Hunter EB, Olson S, Raiford DS. Hepatic stellate cell activation in nonalcoholic steatohepatitis and fatty liver. Hum Pathol 2000;31:822–8.
28. Kasai H. Analysis of a form of oxidative DNA damage, 8-hydroxy-2′-deoxyguanosine, as a marker of cellular oxidative stress during carcinogenesis. Mutat Res 1997;387:147–63.
29. Kleiner DE, Brunt EM, Van Natta M, Behling C, Contos MJ, Cummings OW, et al. Design and validation of a histological

scoring system for nonalcoholic fatty liver disease. Hepatology 2005;41:1313–21.
30. Fromenty B, Pessayre D. Inhibition of mitochondrial beta-oxidation as a mechanism of hepatotoxicity. Pharmacol Ther 1995;67:101–54.
31. Chitturi S, Abeygunasekera S, Farrell GC, Holmes-Walker J, Hui JM, Fung C, et al. NASH and insulin resistance: insulin hypersecretion and specific association with the insulin resistance syndrome. Hepatology 2002;35:373–9.
32. Pagano G, Pacini G, Musso G, Gambino R, Mecca F, Depetris N, et al. Non-alcoholic steatohepatitis, insulin resistance, and metabolic syndrome: further evidence for an etiologic association. Hepatology 2002;35:367–72.
33. Sanyal AJ, Campbell-Sargent C, Mirshahi F, Rizzo WB, Contos MJ, Sterling RK, et al. Non-alcoholic steatohepatitis: association of insulin resistance and mitochondrial abnormalities. Gastroenterology 2001;120:1183–92.
34. Rinella ME, Green RM. The methionine–choline deficient dietary model of steatohepatitis does not exhibit insulin resistance. J Hepatol 2004;40:47–51.
35. Chen A, Zhang L, Xu J, Tang J. The antioxidant (–)-epigallocatechin-3-gallate inhibits activated hepatic stellate cell growth and suppresses acetaldehyde-induced gene expression. Biochem J 2002;368:695–704.
36. Pietrangelo A. Metals, oxidative stress, and hepatic fibrogenesis. Semin Liver Dis 1996;16:13–30.
37. Stärkel P, Sempoux C, Leclercq I, Herin M, Deby C, Desager JP, et al. Oxidative stress, KLF6 and transforming growth factor-β up-regulation differentiate non-alcoholic steatohepatitis progressing to fibrosis from uncomplicated steatosis in rats. J Hepatol 2003;39:538–46.
38. Matsuoka M, Tsukamoto H. Stimulation of hepatic lipocyte collagen production by Kupffer cell-derived transforming growth factor β: implication for a pathogenetic role in alcoholic liver fibrogenesis. Hepatology 1990;11:599–605.
39. Nakatsukasa H, Nagy P, Everts RP, Hsia CC, Marsden E, Thorgeirsson SS. Cellular distribution of transforming growth factor-β1 and procollagen types I, III, and IV transcripts in carbon tetrachloride-induced rat liver fibrosis. J Clin Invest 1990;85:1833–43.